Polyhedron 51 (2013) 292–297

Contents lists available at SciVerse ScienceDirect

Polyhedron

journal homepage: www.elsevier.com/locate/poly

# New ruthenium(II)/phosphines/diimines complexes: Promising antitumor (human breast cancer) and *Mycobacterium tuberculosis* fighting agents

Edjane R. dos Santos [a], Melina A. Mondelli [a], Lucas V. Pozzi [a], Rodrigo S. Corrêa [a], Heloisa S. Salistre-de-Araújo [b], Fernando R. Pavan [c], Clarice Q.F. Leite [c], Javier Ellena [d], Valéria R.S. Malta [e], Sérgio P. Machado [f], Alzir A. Batista [a,*]

[a] Departamento de Química, Universidade Federal de São Carlos, CEP 13565-905 São Carlos, SP, Brazil
[b] Departamento de Ciências Fisiológicas, Universidade Federal de São Carlos, CP 676, CEP 13565-905 São Carlos, SP, Brazil
[c] Departamento de Ciências Biológicas, Faculdade de Ciências Farmacêuticas, UNESP, CEP 14800-900 Araraquara, SP, Brazil
[d] Instituto de Física de São Carlos, Universidade de São Paulo, CEP 13560-970 São Carlos, SP, Brazil
[e] Departamento de Química,Universidade Federal de Alagoas, CEP 57072-970 Maceio, AL, Brazil
[f] Departamento de Química Inorgânica, Instituto de Química, Universidade Federal do Rio de Janeiro, CEP 21941-909 Rio de Janeiro, RJ, Brazil

ARTICLE INFO

*Article history:*
Received 31 October 2012
Accepted 7 January 2013
Available online 17 January 2013

*Keywords:*
Ruthenium(II) complexes
Phosphine/diimine complexes
Cytotoxity
Antimycobacterial activity

ABSTRACT

The synthesis and characterization of ruthenium compounds of the type $[RuCl_2(P)_2(N–N)]$ $[(P)_2 = (PPh_3)_2$, dppb = 1,4-bis(diphenylphosphino)butano; dppp = 1,3-bis(diphenylphosphino)propane; N–N = 5,5′-dimethyl-2,2′dipyridyl (5,5′-mebipy) or 4,4′-dimethyl-2,2′dipyridyl (4,4′-mebipy)] are described. The complexes were characterized using elemental analysis, UV–Vis and infrared spectroscopies, cyclic voltammetry, and X-ray crystallography. *In vitro* evaluation of the complexes, using the MTT methodology, revealed their cytotoxic activities in a range of 5.4–15.7 μM against the MDA-MB-231 breast tumor cells and showed that, in this case, they are more active than the reference metallodrug cisplatin. The *in vitro* antimycobacterial activities of the complexes had their Minimum Inhibitory Concentration (MIC) for MTB cell growth measured, by the REMA method. The MICs for these complexes were found to be between 12.5 and 25.0 μg/mL. The results are comparable with the "second line" drug cycloserine (MIC = 12.5–50.0 μg/mL), commonly used in the treatment of TB.

© 2013 Elsevier Ltd. All rights reserved.

## 1. Introduction

Since the discovery of the cisplatin as an antitumor agent in the sixties, extensive research with transition metal ions has been done and ruthenium has attracted a considerable interest as the basis for new potential metallodrugs to treat cancer diseases [1–3]. Metallopharmaceuticals have enormous potential to help overcome the limitations of current therapies in cancer due to their variety of geometries and chemical reactivities [4]. The activities of these compounds depend on the metal ion, their ligands and the structure of the compounds. Thus, NAMI-A, imidazolium *trans*-[tetrachloro(dimethylsulfoxide)(1H-imidazole)ruthenate(III)], and KP1019, indazolium *trans*-[tetrachlorobis(1H-indazole) ruthenate(III)], are potential antitumor drugs that are in clinical trials having successfully completed phase I. The success of these two compounds reinforces the scope to continue searching for new drugs that may have the cure, or for diminishing unwanted effects of cancer treatment. Also, the bifunctional complexes of the general structural composition $[Ru(\eta^6\text{-arene})X_2(PTA)]$ (PTA = 1,3,5-triaza-7-phosphaadamantane) (RAPTA) showed antimetastatic properties and generally low toxicity comparable to those observed for NAMI-A [3].

The interest in synthesizing new metal compounds is in diminishing the diverse side effects, as nephrotoxicity, toxicity, nausea and vomiting, in cancer patients treated with the cisplatin. In the last five years we have been synthesizing some ruthenium/phosphine/diimine complexes, which are showing promising activity against cancer and also against *Mycobacterium tuberculosis* [MT] [5–9]. The bacterium *M. tuberculosis* is the tuberculosis agent, which is responsible for the death of about 2 million people annually [10]. The treatment of the illness is expensive, long, causes some side effects and encounters resistance. Therefore many researchers are looking for new alternatives in the treatment of this illness such as some ruthenium and gold complexes that have been found to be very promising, showing minimum inhibitory concentrations (MICs) comparable to or even better than some reference drugs used in the treatment of tuberculosis [7–9,10].

In this work, four new ruthenium complexes were synthesized, characterized, their X-rays structures were determined, and their

* Corresponding author.
*E-mail address:* daab@ufscar.br (A.A. Batista).

0277-5387/$ - see front matter © 2013 Elsevier Ltd. All rights reserved.
http://dx.doi.org/10.1016/j.poly.2013.01.004

citotoxicity tested against MDA-MB-231 (human breast cancer) cancer cells and against MT.

## 2. Experimental

### 2.1. Materials and measurements

All manipulations were carried out under purified argon using standard Schlenk techniques. Reagent grade solvents were appropriately distilled and dried before use. All chemicals used were of reagent grade or comparable purity. All chemicals were purchased from Aldrich or Fluka and were used as received. The precursors $[RuCl_2(PPh_3)_3]$ and $[RuCl_2(dppb)(PPh_3)]$ were prepared using published procedures [11–13].

The IR spectra of the complexes were recorded on a FTIR Bomem-Michelson 102 spectrometer in the 4000–200 $cm^{-1}$ region using solid samples pressed in CsI pellets. The NMR spectra of $^{31}P\{^1H\}$ were recorded using a BRUKER, DRX400 tesla equipment, in a BBO 5 mm probe at room temperature, and dichloromethane was used as solvent, using a capillary containing D2O. The molar conductance measurements ($\Lambda$) were carried out in dichloromethane at 25 °C, using concentrations of $1.0 \times 10^{-3}$ M for the complexes. Cyclic voltammetry (CV) experiments were carried out at room temperature in $CH_2Cl_2$ containing 0.100 M $Bu_4NClO_4$ (TBAP) (Fluka Purum) using a BAS-100B/W Bioanalytical Systems Instrument. The working and auxiliary electrodes were stationary Pt foils; the reference electrode was of Ag/AgCl, in a Luggin capillary probe. The electronic spectra were obtained through a scanning done on a Hewlett–Packard diode array, model 8452A, spectrophotometer. The microanalyses were performed at the Microanalytical Laboratory at the Federal University of São Carlos, São Carlos, São Paulo, using a FISIONS CHNS, mod. EA 1108 micro analyzer.

### 2.2. Synthesis

#### 2.2.1. Synthesis of $[RuCl_2(PPh_3)_2(5,5'\text{-mebipy})]$ (**1**)

The complex was obtained by reacting 0.500 g (0.520 mmol) of $[RuCl_2(PPh_3)_3]$ dissolved in 20.0 mL of dichloromethane, previously deaerated, and after that 0.106 g (0.570 mmol) of 5,5′-mebipy was added. For the syntheses of the complex (**1**) and (**2**) the solutions were refluxed for 2 h, after that the volumes were diminished until 2 mL and diethyl ether was added for the precipitation of the desired product. The solids were filtered off, well rinsed with diethyl ether (3 × 5 mL) and dried in vacuum. Yield 0.413 g (90%) Experimental *Anal.* Calc. for $C_{48}H_{42}P_2N_2Cl_2Ru$: C, 65.84; H, 4.66; N, 3.22. Found: C, 65.46; H, 4.81; N, 3.18%. Molar conductance (μS/cm, $CH_2Cl_2$) 3.2. $^{31}P\{^1H\}$ NMR (162 MHz, $CH_2Cl_2/D_2O$) $\delta$(ppm) 27.6 (s) Selected IR($cm^{-1}$; w = weak; s = strong): 1604 [w, $\nu$(C=N)], 1481[s, $\nu$(C=N)], 1435 [s, $\nu$(C=N)], 517 [s, $\nu$(Ru–P)], 461 [w, $\nu$(Ru–N)], 303 e 287 [w, $\nu$(Ru–Cl)]. UV–Vis, $CH_2Cl_2$ $\lambda_{max}$/nm ($\varepsilon/M^{-1}\,cm^{-1}$): 272 (22 391), 306 (21 361), 460 (1458).

#### 2.2.2. Synthesis of cis-$[RuCl_2(dppb)(5,5'\text{-mebipy})]$ (**2**)

The complex was obtained by reacting 0.300 g (0.350 mmol) of $[RuCl_2(dppb)(PPh_3)]$ dissolved in 20.0 mL of dichloromethane, previously deaerated, and after that 0.071 g (0.380 mmol) of 5,5′-mebipy was added. Yield 0.246 g (90%). Experimental *Anal.* Calc. for $C_{40}H_{40}Cl_2N_2P_2Ru$: C, 61.24; H, 5.22; N, 3.68. Found: C, 61.38; H, 5.15; N, 3.58%. Molar conductance (μS/cm, $CH_2Cl_2$) 4.5. $^{31}P\{^1H\}$ NMR (162 MHz, $CH_2Cl_2/D_2O$) $\delta$(ppm) 45.4 (d) and 31.8 (d) $^2J_{p-p}$(Hz) 32.7. Selected IR($cm^{-1}$): 1637 [w, $\nu$(C=N)], 1475 [s, $\nu$(C=N)], 1433 [s, $\nu$(C=N)], 519 [s, $\nu$(Ru–P)], 436 [w, $\nu$(Ru–N)], 301 e 267 [w, $\nu$(Ru–Cl)]. UV–Vis $CH_2Cl_2$ $\lambda_{max}$/nm ($\varepsilon/M^{-1}\,cm^{-1}$): 312 (16594), 424 (2330).

#### 2.2.3. Synthesis of cis-$[RuCl_2(dppp)(N–N)]$; N–N = 5,5′-mebipy (**3**) or (4,4′-mebipy) (**4**)

These complexes were synthesized by reacting 0.300 g (0.340 mmol) of $[RuCl_2(PPh_3)_2(N–N)]$, [N–N = 5,5′-mebipy (**3**) or 4,4′-mebipy (**4**)] in 30.0 mL of a mixture of dichlorometane:benzene (1:1) with 0.210 g (0.510 mmol) of dppp [1,3-bis(diphenilphosphine) propane]. For the syntheses of the complex (**3**) and (**4**) the solutions were refluxed for 4 days. (**3**): Yield: 0.223 g (85%). Experimental *Anal.* Calc. for $C_{39}H_{38}Cl_2N_2P_2Ru$: C, 60.90; H, 5.27; N, 3.27. Found: C, 60.94; H, 4.98; N, 3.64%. Molar conductance (μS/cm, $CH_2Cl_2$) 1.7. $^{31}P\{^1H\}$ NMR (162 MHz, $CH_2Cl_2/D_2O$) $\delta$(ppm) 38, (d) and 30.2 (d) $^2J_{p-p}$(Hz) 42,2. Selected IR ($cm^{-1}$): 1618 [w, $\nu$(C=N)], 1483 [s, $\nu$(C=N)], 1433 [s, $\nu$(C=N)], 517 [s, $\nu$ (Ru–P)], 444 [w, $\nu$(Ru–N)], 301 and 274 [w, $\nu$(Ru–Cl)]. UV–Vis $CH_2Cl_2$, $\lambda_{max}$/nm ($\varepsilon/M^{-1}\,cm^{-1}$): 292 (13885), 424 (1954).

(**4**): Yield: 0.236 g (90%). Experimental *Anal.* Calc. for $C_{39}H_{38}Cl_2N_2P_2Ru$: C, 61.05; H, 5.01; N, 3.40. Found: C, 60.94; H, 4.98; N, 3.64%. Molar conductance (μS/cm, $CH_2Cl_2$) 2.0. $^{31}P\{^1H\}$ NMR (162 MHz, $CH_2Cl_2/D_2O$) $\delta$(ppm) 39.3 (d) and 28.8 (d) $^2J_{p-p}$(Hz) 42.0.Selected IR($cm^{-1}$): 1585 [w, $\nu$ (C=N)], 1481[s, $\nu$(C=N)], 1433 [s, $\nu$(C=N)], 515 [s, $\nu$(Ru–P)], 442 [w, $\nu$(Ru–N)], 303 e 276 [w, $\nu$(Ru–Cl)]. UV–Vis $CH_2Cl_2$ $\lambda_{max.}$/nm ($\varepsilon/M^{-1}\,cm^{-1}$): 306 (14252), 424 (1947).

### 2.3. Cell culture assay in MDA-MB-231

*In vitro* cytotoxicity assays on cultured human tumor cell lines still represent the standard method for the initial screening of antitumoral agents. Thus, as a first step in assessing their pharmacological properties, the new ruthenium complexes were assayed against a human breast tumor cell line MDA-MB-231 (ATCC No. HTB-26). The cells were routinely maintained in Dulbecco's Modified Eagle's medium (DMEM) supplemented with 10% fetal bovine serum (FBS), at 37 °C in a humidified 5% $CO_2$ atmosphere. After reaching confluence, the cells were detached by trypsinization and counted. For the cytotoxicity assay, $5 \times 10^4$ cells $well^{-1}$ were seeded in 200 μL of complete medium in 96-well assay microplates (Corning Costar). The plates were incubated at 37 °C in 5% $CO_2$ for 24 h to allow cell adhesion, prior to drug testing. All tested compounds were dissolved in sterile DMSO (stock solution with maximum concentration of 20 mM) and diluted to 5, 2, 1, 0.5, 0.2, 0.02 and 0.002 mM. From each of these dilute samples 2 μL aliquots were added to 200 μL medium (without FBS) giving a final concentration of DMSO of approximately 1% and a final concentration of the complex diluted about 100 times. Cells were exposed to the compounds for a 24 h-period. Cell respiration, as an indicator of cell viability, was determined by the mitochondrial-dependent reduction of MTT [3-(4,5-dimethylthiazol-2-yl)-2,5-diphenyl tetrazolium bromide] to formazan [14]. MTT solution (0.5 mg/mL) was added to cell cultures and incubated for 3 h, after which 100 μL of isopropanol was added to dissolve the precipitated formazan crystals. The conversion of MTT to formazan by metabolically viable cells was monitored in an automated microplate reader at 570 nm. The percent cell viability was calculated by dividing the average absorbance of the cells treated with the test compounds by that of the control; % cell viability was plotted against drug concentration (logarithmic scale) to determine the $IC_{50}$ (drug concentration at which 50% of the cells are viable relative to the control), with the error estimated from the average of three trials.

### 2.4. Antimycobacterial activity assay

Antimycobacterial activities of each tested compound and of the standard drug isoniazide (Difco laboratories, Detroit, MI, USA) were determined in triplicate in 96 sterilized flat bottomed micro-plates (Falcon 3072; Becton Dickinson, Lincoln Park, NJ, USA) and Middlebrook 7H9 Broth (Difco) supplemented with oleic

**Table 1**
Crystal data and structure refinement for the complexes (**2**) *cis*-[$RuCl_2$(dppb)(5,5′-mebipy)], (**3**) *cis*-[$RuCl_2$(dppp)(5,5′-mebipy)] and (**4**) *cis*-[$RuCl_2$(dppp)(4,4′-mebipy)].

| Empirical formula | **$C_{40}H_{40}Cl_2N_2P_2Ru$(2)** | **$C_{39}H_{38}Cl_2N_2P_2Ru{\cdot}CH_2Cl_2$(3)** | **$C_{39}H_{38}Cl_2N_2P_2Ru$(4)** |
|---|---|---|---|
| Formula weight | 782.65 | 853.55 | 768.62 |
| Temperature(K) | 298(2) | 298(2) | 298(2) |
| Crystal system | Monoclinic | Triclinic | Monoclinic |
| Space group | $P2_1/c$ | P-1 | $P2_1/c$ |
| *Unit cell dimensions* | | | |
| (*a*) (Å) | 17.2615(2) | 10.3775(9) | 11.7965(1) |
| (*b*) (Å) | 12.5182(1) | 11.797(1) | 13.0803(2) |
| (c) (Å) | 17.9871(2) | 16.787(1) | 24.0323(4) |
| ($\alpha$) (°) | 90 | 80.466(4) | 90 |
| ($\beta$) (°) | 111.949(1) | 75.158(3) | 97.8870(10) |
| ($\gamma$) (°) | 90 | 78.196(4) | 90 |
| Volume (Å$^3$) | 3604.98(6) | 1930.6(3) | 3673.15(9) |
| *Z* | 4 | 2 | 4 |
| Density (calc) (Mg/m$^3$) | 1.442 | 1.468 | 1.39 |
| Absorption coefficient (mm$^{-1}$) | 0.703 | 0.797 | 0.689 |
| *F*(000) | 1608 | 872 | 1576 |
| Crystal size (mm$^3$) | 0.50 × 0.17 × 0.07 | 0.20 × 0.11 × 0.10 | 0.08 × 0.17 × 0.18 |
| Theta range for data collection (°) | 3.02–26.71 | 3.08–26.39 | 3.00–26.73 |
| Index ranges | $-2l \leqslant h \leqslant 2l$, $-15 \leqslant k \leqslant 15$, $-22 \leqslant l \leqslant 22$ | $-12 \leqslant h \leqslant 12$, $-14 \leqslant k \leqslant 14$, $-20 \leqslant l \leqslant 20$ | $-14 \leqslant h \leqslant 14$, $-16 \leqslant k \leqslant 16$, $-29 \leqslant l \leqslant 30$ |
| Reflections collected | 27579 | 14706 | 26976 |
| Independent reflections | 7570, R(int) (0.0381) | 7843, R(int) (0.0296) | 7759, R(int) (0.0491) |
| Maximum and minimum transmission | 0.956 and 0.643 | 0.923 and 0.864 | 0.9544 and 0.9006 |
| Final *R* indices [$I > 2\sigma(I)$] | $R_1$ = 0.0365, $wR_2$ = 0.0955 | $R_1$ = 0.0505, $wR_2$ = 0.1162 | $R_1$ = 0.0393, $wR_2$ = 0.0911 |
| *R* indices (all data) | $R_1$ = 0.0448, $wR_2$ = 0.1012 | $R_1$ = 0.0624, $wR_2$ = 0.1254 | $R_1$ = 0.0602, $wR_2$ = 0.0966 |
| Largest diffraction in peak and hole (e Å$^{-3}$) | 0.500 and −0.740 | 0.576 and −0.704 | 0.396 and −0.789 |
| Goodness-of-fit (GOF) on $F^2$ | 1.034 | 1.134 | 1.003 |

acid–albumin–dextrose–catalase (OADC) enrichment (BBL/Becton Dickinson, Sparks, MD, USA). The concentrations of the tested compound ranged from 0.15 to 250 μg/mL and the isoniazide ranged from 0.015 to 1.0 μg/mL. The micro-plate Alamar Blue assay [11] (MABA) was used to measure the minimal inhibitory concentration (MIC) for the tested compounds (minimum concentration necessary to inhibit 90% growth of *M. tuberculosis* $H_{37}$Rv ATCC 27294). The development of the color pink, in the wells, was taken as an indicator of bacterial growth and the maintenance of the color blue as the contrary. Thus, the MIC was assumed to be the lowest concentration able to inhibit the change of color from blue to pink. MIC values were determined by fluorescence measured on a SPECTRAfluor Plus microfluorimeter (Tecan®), with excitation at 530 nm and emission at 590 nm.

### 2.5. X-ray diffraction data

The crystals of the complexes were grown by slow evaporation of the solutions in dichloromethane/diethyl ether. Suitable yellow crystals of complexes were grown by the diffusion of diethyl ether into a dichloromethane solution of the complex. Crystals were measured on an Enraf–Nonius KappaCCD diffractometer, using a wavelength of 0.71073 (Å).

The final unit cell parameters were based on all reflections. Data collections were made using the COLLECT program [15]; integration and scaling of the reflections were performed with the HKL DENZO-SCALEPACK system of programs [16]. Absorption corrections were carried out using the Gaussian method [17]. The structures were solved by direct methods using the SHELXS-97 [18]. The model was refined by using the least-squares full-matrix on $F^2$ by means of SHELXL-97 [19]. The ORTEP views of the structures were prepared using the ORTEP-3 for WINDOWS [20]. All the hydrogen atoms were stereochemically positioned and refined with the riding model. All H atoms were located on stereochemical grounds. Data collections and experimental details for the complexes are summarized in Table 1. Relevant interatomic bond lengths and angles are listed in Table 2.

**Table 2**
Selected bond distances (Å) and bond angles (°) for the (**2**), (**3**) and (**4**) complexes.

| Distance (°) | (**2**) | (**3**) | (**4**) |
|---|---|---|---|
| Ru–N(1) | 2.115(2) | 2.095(3) | 2.071(2) |
| Ru–N(2) | 2.134(2) | 2.110(3) | 2.107(2) |
| Ru–P(1) | 2.3016(6) | 2.2686(9) | 2.2719(7) |
| Ru–P(2) | 2.3189(6) | 2.3150(9) | 2.3278(7) |
| Ru–Cl(1) | 2.4237(6) | 2.4361(8) | 2.4378(7) |
| Ru–Cl(2) | 2.4614(6) | 2.4882(9) | 2.4940(7) |
| N(1)–Ru–N(2) | 77.25(8) | 77.55(11) | 77.89(8) |
| N(1)–Ru–P(1) | 98.85(5) | 94.14(8) | 95.61(6) |
| N(2)–Ru–P(1) | 91.40(6) | 91.84(8) | 91.53(6) |
| N(1)–Ru–P(2) | 102.40(5) | 107.29(8) | 102.19(6) |
| N(2)–Ru–P(2) | 173.24(6) | 173.24(8) | 173.34(6) |
| P(1)–Ru–P(2) | 95.31(2) | 92.50(3) | 95.08(3) |
| N(1)–Ru–Cl(1) | 165.41(6) | 169.49(8) | 170.58(6) |
| N(1)–Ru–Cl(2) | 83.43(5) | 84.08(8) | 83.49(6) |
| N(2)–Ru–Cl(1) | 89.08(6) | 91.94(8) | 92.72(6) |
| N(2)–Ru–Cl(2) | 85.53(6) | 83.50(8) | 83.94(6) |
| P(1)–Ru–Cl(1) | 86.42(2) | 85.86(3) | 85.13(3) |
| P(2)–Ru–Cl(2) | 87.72(2) | 83.20(3) | 89.45(3) |
| Cl(1)–Ru–Cl(2) | 90.52(2) | 95.09(3) | 95.03(3) |

### 2.6. Theoretical calculations

The geometry optimization was performed using a i-7 computer, with a GAUSSIAN 09 programXX with the B3LYP hybrid density functional combined with the 6-31G(d,p) and LACVP* basis set and for Ru atoms. The calculation of frequencies used to find the minimum geometries does not have imaginary values [21].

## 3. Results and discussion

### 3.1. Syntheses of the complexes

The molar conductance measurements for the prepared complexes (**1**–**4**) were carried out in dichloromethane and the results are consistent with neutral type compounds [22].

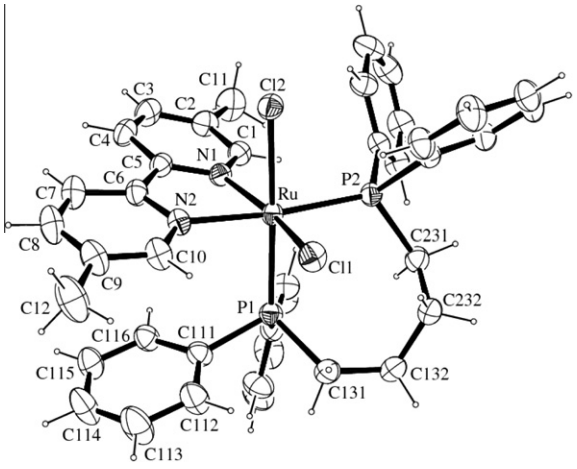


**Fig. 1.** ORTEP View of *cis*-[$RuCl_2$(dppb)(5,5′-mebipy)] (**2**) showing the atom-labeling scheme and the 30% probability thermal ellipsoids.

### 3.2. Structural studies

The ORTEP diagrams of the complexes are shown in Figs. 1–3. In the structures, the metal displays the expected distorted octahedral coordination geometry.

For all three structures the distances of Ru–P(2) (phosphorus atoms *trans* to nitrogen) are longer than the distances of Ru–(P1) (phosphorus atoms *trans* to chloride). This can be a consequence of the competitive effect between the phosphorus and the nitrogen atoms, two π acceptor species, for the electronic density of the ruthenium. This has also been observed in other ruthenium complexes [23]. Also, the distances Ru–Cl(2) *trans* to phosphorus atoms are longer than the ones in which the chlorides are *trans* to the nitrogen atoms, Ru–Cl(1), which is a consequence to the strong *trans* effect of the phosphorus atoms [24,25]. Another observation is with respect to the *trans* Ru–Cl bond length, where the chloride is *trans* to the phosphorus atoms. Thus, for the *cis*-$RuCl_2$(dppp)(5,5′-mebipy), Ru(1)–Cl(2) = 2.4882(9) Å and for the *cis*-$RuCl_2$(dppp)(4,4′-mebipy), Ru(1)–Cl(2) = 2.4940(7) Å these distances are only slightly longer than the Ru–Cl distance in the *cis*-$RuCl_2$(dppb)(5,5′-mebipy), Ru(1)–Cl(2) = 2.4614(6) Å, but consistent with the higher basicity of the dppb ($pK_a$ = 4.72), when compared with the basicity of the dppp ($pK_a$ = 4.50) [26,27].

### 3.3. Spectroscopical characterization

The $^{31}P\{^1H\}$ NMR spectra of the new compounds present a typical AX pattern, which corresponds to the observation of two doublets in the spectrum. Then, differently from the precursor complex, which the NMR $^{31}P\{^1H\}$ presents a singlet in 27.6 ppm, the new diphosphine derivatives have magnetic nonequivalent phosphorus atoms (P *trans* Cl and P *trans* L). It is suggested that the most unshielded signal refers to the phosphorous *trans* to the nitrogen of the pyridines, and the most shielded signal, which is close to that observed for similar complexes, refers to the phosphorous *trans* to Cl atom (see Table 3) [28].

The IR spectra of the new complexes confirm the presence of the ligands coordinated to the metal. The presence of two *ν*(Ru–Cl) bands in the IR spectra of the complexes supports the *cis* position of the chlorine in their structures, as shown by the X-ray technique. The electronic spectra of the complexes show a band [two bands for the complex (**1**)] in the UV region, which can be attributed to the intra-ligand transitions ($\pi \rightarrow \pi^*$) from its comparison to the UV spectra of free ligands ($PPh_3$, dppp, dppb, 4,4′-mebipy and 5,5′-mebipy), and a second band that corresponds to the charge transfer transition (MLCT) of the metal to the ligand, at lower energies [29,30].

### 3.4. Electrochemical behavior

The results of the cyclic voltammetry measurements for the complexes (**1**–**4**), in $CH_2Cl_2$ solutions, at room temperature, are presented in Table 4 and Fig. 4. The complexes (**1**–**4**) showed quasi-reversible processes, corresponding to a one-electron redox process $Ru^{III}/Ru^{II}$.

A general trend is that complexes containing monodentate phosphine ligands show lower oxidation potentials when compared to similar complexes containing bidentate ligands, with similar basicity. This can be explained by the strong competition between the *trans* π acceptor atoms for the same *d* electrons of the metallic center (*trans* competitive effect) [30–32].

As can be seen in Table 4 the redox potentials of the complexes follow the basicity of the bipyridine or of the diphosphine ligands, and in Fig. 5 there is a good correlation between the values plotted for the redox potentials of the complexes and the Mulliken charges on the ruthenium atom (% of Ru d-orbitals): −0.104, −0.099 and −0.091, for *cis*-[$RuCl_2$(dppb)(5,5′-mebipy)], *cis*-[$RuCl_2$(dppp)(5,5′-mebipy)] and *cis*-[$RuCl_2$(dppp)(4,4′-mebipy)], respectively.

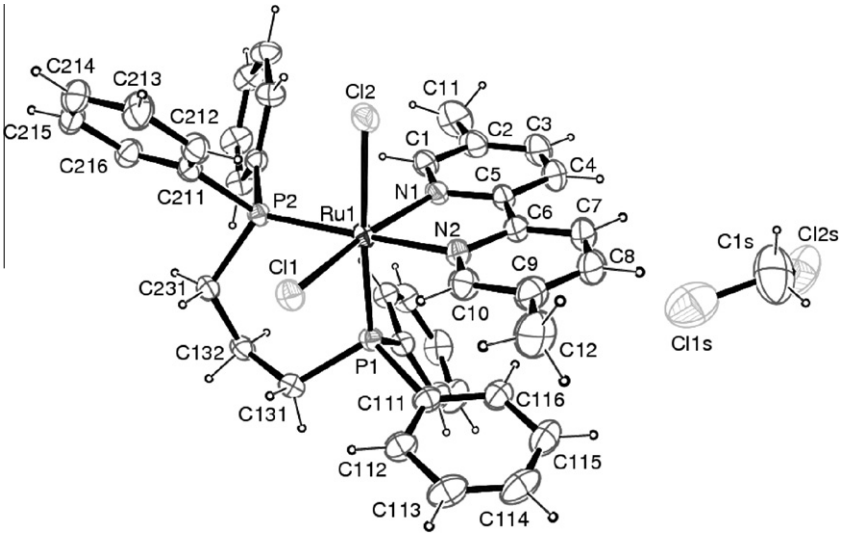


**Fig. 2.** ORTEP View of *cis*-[$RuCl_2$(dppp)(5,5′-mebipy)]·$CH_2Cl_2$ (**3**), showing the atom-labeling scheme and the 30% probability thermal ellipsoids.

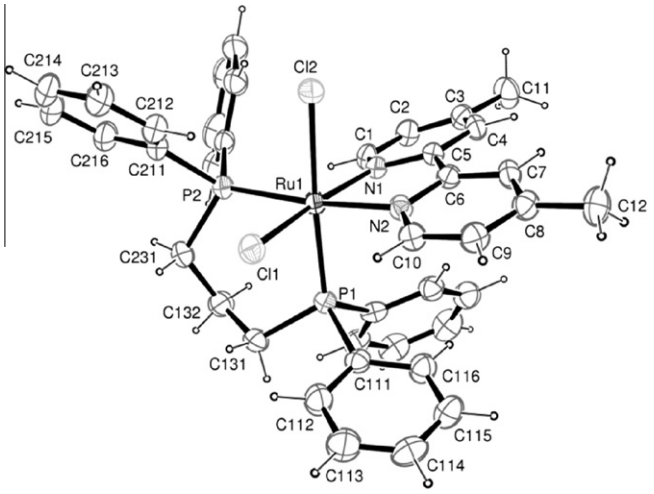


**Fig. 3.** ORTEP View of *cis*-[$RuCl_2$(dppp)(4,4′-mebipy)] (**4**) showing the atom-labelingscheme and the 30% probability thermal ellipsoids.

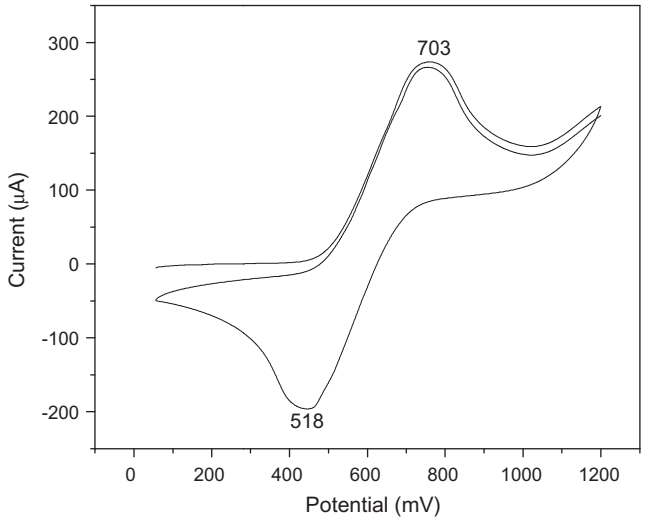


**Fig. 4.** The cyclic voltammogram of the *cis*-[$RuCl_2$(dppp)(5,5′-mebipy)] complex: TBAP 0.1 mol $L^{-1}$; $CH_2Cl_2$; Ag/AgCl; scan rate of 100 mV $s^{-1}$.

**Table 3**
$^{31}P\{^1H\}$ NMR data of ruthenium containing compounds, in $CH_2C_{l2}$.

| Complexes | ($\delta$) | $^2Jp\text{-}_p$(Hz) |
|---|---|---|
| *cis,trans*-[$RuCl_2(PPh_3)2$(5,5′-mebipy)] | 27.6 | – |
| *cis*-[$RuCl_2$(dppb)(5,5′-mebipy)] | 45.4 e 31.8 | 32.7 |
| *cis*-[$RuCl_2$(dppp)(5,5′-mebipy)] | 39.3 e 28.8 | 42.0 |
| *cis*-[$RuCl_2$(dppp)(4,4′-mebipy)] | 38.8 e 30.2 | 42.2 |

**Table 4**
Electrochemical data for the complexes (1–4), scan rate of 100 mV/s∗.

| Complex | $E_{1/2}$ (mV) | *E*pa (mV) | *E*pc (mV) | *I*pa/ *I*pc |
|---|---|---|---|---|
| *cis,trans*-[$RuCl_2(PPh_3)2$(5,5′-mebipy)] | 340 | 379 | 303 | 1.1 |
| *cis*-[$RuCl_2$(dppb)(5,5′-mebipy)] | 625 | 670 | 580 | 1.0 |
| *cis*-[$RuCl_2$(dppp)(5,5′-mebipy)] | 610 | 703 | 518 | 1.0 |
| *cis*-[$RuCl_2$(dppp)(4,4′-mebipy)] | 600 | 754 | 445 | 1.3 |

p$K_a$ of the ligands: dppb = 4.72 ; dppp = 4.50 ; 4,4′-mebipy = 4.92 ; 5,5′-mebipy = 5.01.

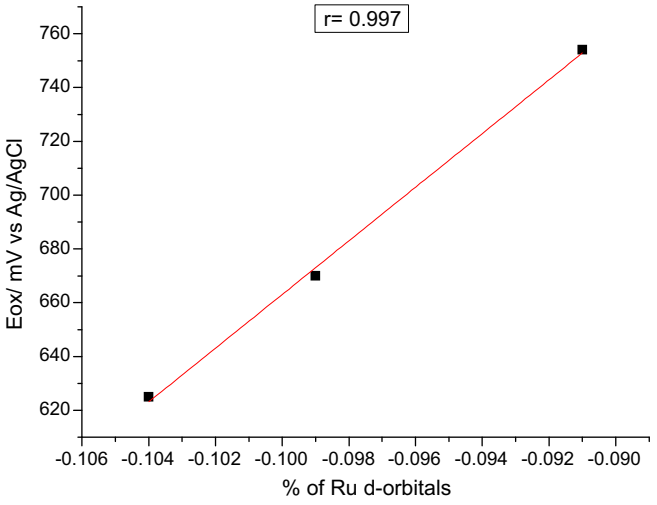


**Fig. 5.** Relationship between the oxidation potential [*E*pa(mV)] values of the complexes vs. Mulliken charges on their metal centers.

### 3.5. Antitumor activity

The MDA-MB-231 tumor cell line (human breast carcinoma) was exposed to (2–4) compounds for a period of 48 h in order to allow them to reach their biological target. The $IC_{50}$ (drug concentration at which 50% of the cells are viable relative to the control) values, calculated from the dose-survival curves obtained after 48 h of drug treatment with an MTT assay, are shown in Table 5. For comparison purposes, the cytotoxicity of cisplatin was evaluated under the same experimental conditions.

The complexes showed a good activity against human MDA-MB-231 cell lines, compared to cisplatin these complexes are 4 to 10-fold more active in fighting MDA-MB-231, indicating their potentiality as anti-tumor agents.

**Table 5**
$IC_{50}$ values for the MDA-MB-231 cell line of Ru(II) complexes (1–4), and the cisplatin measured in a DMSO solution.

| Complex | $IC_{50}$ μmol $L^{-1}$ |
|---|---|
| *cis,trans*-[$RuCl_2(PPh_3)_2$(5,5′-mebipy)] | 10.31 ± 0.21 |
| *cis*-[$RuCl_2$(dppb)(5,5′-mebipy)] | 5.41 ± 0.71 |
| *cis*-[$RuCl_2$(dppp)(5,5′-mebipy)] | 14.60 ± 1.81 |
| *cis*-[$RuCl_2$(dppp)(4,4′-mebipy)] | 15.64 ± 0.44 |
| $PPh_3$ | 27.2 ± 0.49 |
| dppp | 10.59 ± 0.91 |
| dppb[9] | >200 |
| 4,4′-Mebipy[9] | >200 |
| 5,5′-Mebipy | >200 |
| Cycloserine | 63.0 ± 5.0 |

### 3.6. Antimicobacterial activity

The *in vitro* anti-*M. tuberculosis* properties of the free ligands dppp, dppb and the precursors used to synthesize the complexes *cis*-[$RuCl_2$(dppb)(5,5′-mebipy)], *cis*-[$RuCl_2$(dppp)(5,5′-mebipy)] and *cis*-[$RuCl_2$(dppp)(4,4′-mebipy)], were tested against *M. tuberculosis* $H_{37}$Rv ATCC 27294, the observed MICs are reported in Table 6. The values obtained were comparable to cycloserine (MIC 12.5–50.0 μg/mL), an actually used "second line" drug.

**Table 6**
MIC values of anti-*M. tuberculosis* activity of ruthenium complexes, free ligands and reference drugs.

| Complex | MIC (μg/mL) |
|---|---|
| *cis,trans*-[$RuCl_2(PPh_3)_2$(5,5′-mebipy)] | 10.17 |
| *cis*-[$RuCl_2$(dppb)(5,5′-mebipy)] | 25.00 |
| *cis*-[$RuCl_2$(dppp)(5,5′-mebipy)] | 12.50 |
| *cis*-[$RuCl_2$(dppp)(4,4′-mebipy)] | 12.50 |
| $PPh_3$ | 25 |
| dppp | >50 |
| dppb[9] | >50 |
| 4,4′-Mebipy[9] | 25 |
| 5,5′-Mebipy | 27 |
| Cycloserine | 12.5–50.0 |
| Isoniazide | 0.03 |

## 4. Conclusions

Four new ruthenium(II)/phosphines/diimines compounds were synthesized, characterized and their biological activity evaluated. The $IC_{50}$ values for the MDA-MB-231 cell line of Ru(II) complexes showed better activity than the cisplatin (reference drug), and the MIC values of anti-*M. tuberculosis* activity obtained for the complexes showed an activity comparable to cycloserine, a second line drug used in the treatment of the illness. The crystal structures of the [$RuCl_2$(dppb)(5,5′-mebipy)], [$RuCl_2$(dppp)(5,5′-mebipy)] and [$RuCl_2$(dppb)(4,4′-mebipy)] complexes were determined and for all of them the chlorines are in the *cis* position to each other, as suggested by $^{31}P\{^1H\}$ NMR experiments.

## Acknowledgment

We thank CNPq, CAPES, FAPESP, FAPERJ and CYTED, for financial support.

## Appendix Supplementary. material

CCDC 906486, 906487 and 906488 contain the supplementary crystallographic data for *cis*-[$RuCl_2$(dppb)(5,5′-mebipy)], *cis*-[$RuCl_2$(dppp)(5,5′-mebipy)] and *cis*-[$RuCl_2$(dppp)(4,4′-mebipy)] complexes. These data can be obtained free of charge via http://www.ccdc.cam.ac.uk/conts/retrieving.html, or from the Cambridge Crystallographic Data Centre, 12 Union Road, Cambridge CB2 1EZ, UK; fax: +44 1223-336-033; or e-mail: deposit@ccdc.cam.ac.uk.

## References

[1] A. Bergamo, G. Sava, Dalton Trans. 40 (2011) 7817.
[2] A. Bergamo, A. Masi, A.F.A. Peacock, A. Habtemariam, P.J. Sadler, G. Sava, J. Inorg. Biochem. 104 (2010) 79.
[3] P. Nowak-Sliwinska, J.R. van Beijnum, A. Casini, A.A. Nazarov, G. Wagnières, H. van den Bergh, P.J. Dyson, A.W. Griffioen, J. Med. Chem. 54 (2011) 3895.
[4] S. Ahmad, A.A. Isab, S. Ali, A.R. Al-Arfaj, Polyhedron 25 (2006) 1633.
[5] C. Golfeto, G. Von Poelhsitz, H.S. Selistre-de-Araújo, M.P. de Araujo, J. Ellena, E.E. Castellano, L.G.L. França, I.S. Moreira, A.A. Batista, J. Inorg. Biochem. 104 (2010) 489.
[6] T.A. Heinrich, G. Von Poelhsitz, R.I. Reis, E.E. Castellano, A. Neves, M. Lanznaster, S.P. Machado, A.A. Batista, C.M. Costa-Neto, Eur. J. Med. Chem. 46 (2011) 3616.
[7] F.R. Pavan, G. Von Poelhsitz, F.B. do Nascimento, S.R.A. Leite, A.A. Batista, Victor M. Deflon, Daisy N. Sato, S.G. Franzblau, C.Q.F. Leite, Eur. J. Med. Chem. 45 (2010) 598–601.
[8] F.B. Nascimento, G. Von Poelhsitz, F.R. Pavan, D.N. Sato, C.Q.F. Leite, H.S.S. Araujo, J. Ellena, E.E. Castellano, V.M. Deflon, A.A. Batista, J. Inorg. Biochem. 102 (2008) 1783.
[9] F.R. Pavan, G. Von Poelhsitz, M.I.F. Barbosa, S.R.A. Leite, A.A. Batista, J. Ellena, L.S. Sato, S.G. Franzblau, V. Moreno, D. Gambino, C.Q.F. Leite, Eur. J. Med. Chem. 46 (2011) 5099.
[10] Global Alliance for TB Drug Development. www.tballiance.org (accessed 19.07.12).
[11] T.A. Stephenson, G. Wilkinson, J. Inorg. Nucl. Chem. 28 (1966) 945.
[12] S.L. Queiroz, M.P. de Araujo, A.A. Batista, K.S. MacFarlane, B.R. James, J. Chem. Educ. 78 (2001) 87.
[13] M. Bressan, P. Rigo, Inorg. Chem. 14 (1975) 2286.
[14] T. Mosmann, J. Immunol. Methods 65 (1983) 55.
[15] Enraf-Nonius, Collect, Nonius BV, Delft, The Netherlands, 1997–2000.
[16] Z. Otwinowski, W. Minor, Macromol. Crystallogr. Part A 276 (1997) 307.
[17] R.H. Blessing, Acta Crystallogr., Sect. A 51 (1995) 33.
[18] G.M. Sheldrick, SHELXS-97 Program for Crystal Structure Resolution, University of Göttingen, Göttingen, Germany, 1997.
[19] G.M. Sheldrick, ShelXL-97, University of Göttingen, Göttingen, Germany, Program for Crystal Structures Analysis, 1997.
[20] L.J. Farrugia, J. Appl. Crystallogr. 30 (1997) 565.
[21] M.J. Frisch, G.W. Trucks, H.B. Schlegel, G.E. Scuseria, M.A. Robb, J.R. Heeseman, G. Scalmani, V. Barone, B. Mennucci, G.A. Petersson, H. Nakatsuji, M. Caricato, X. Li, H.P. Hratchian, A.F. Izmaylov, J. Bloino, G. Zheng, J.L. Sonnenberg, M. Hada, M. Ehara, K. Toyota, R. Fukuda, J. Hasegawa, M. Ishida, T. Nakajima, Y. Honda, O. Kitao, H. Nakai, T. Vreven, J. A. Montgomery Jr., J.E. Peralta, F. Ogliaro, M. Bearpark, J.J. Heyd, E. Brothers, K.N. Kudin, V.N. Staroverov, R. Kobayashi, J. Normand, K. Raghavachari, A. Rendell, J.C. Burant, S.S. Iyengar, J. Tomasi, M. Cossi, N. Rega, N.J. Millam, M. Klene, J.E. Knox, J.B. Cross, V. Bakken, C. Adamo, J. Jaramillo, R. Gomperts, R.E. Stratmann, O. Yazyev, A.J. Austin, R. Cammi, C. Pomelli, J.W. Ochterski, R.L. Martin, K. Morokuma, V.G. Zakrzewski, G.A. Voth, P. Salvador, J.J. Dannenberg, S. Dapprich, A.D. Daniels, Ö. Farkas, J.B. Foresman, J.V. Ortiz, J. Cioslowski, D.J. Fox, GAUSSIAN, Inc., Wallingford CT, 2009.
[22] W.J. Geary, Coord. Chem. Rev. 7 (1971) 81.
[23] G. Von Poelhsitz, M.P. de Araujo, L.A.A. de Oliveira, S.L. Queiroz, J. Ellena, E.E. Castellano, A.G. Ferreira, A.A. Batista, Polyhedron 21 (2002) 2221.
[24] E.M.A. Valle, B.A.V. Lima, A.G. Ferreira, F.B. do Nascimento, Victor M. Deflon, I.C.N. Diógenes, U. Abram, J. Ellena, E.D. Castellano, A.A. Batista, Polyhedron 28 (2009) 3473.
[25] A.A. Batista, L.A.C. Cordeiro, G. Oliva, O.R. Nascimento, Inorg. Chim. Acta 258 (1997) 131.
[26] S.J. Berners-Price, R.E. Norman, P.J. Sadler, J. Inorg. Biochem. 31 (1987) 197.
[27] J.R. Sowa, R.J. Angelici, J. Inorg. Chem. 30 (1991) 3534.
[28] S.L. Queiroz, A.A. Batista, G. Oliva, M.T. do P. Gambardella, R.H.A. Santos, K.S. MacFarlane, S.J. Rettig, B.R. James, Inorg. Chim. Acta 267 (1998) 209.
[29] J. Chakravarty, S. Bhattacharya, Polyhedron 13 (1994) 2671.
[30] B. Sullivan, D. Salmon, T. Meyer, Inorg. Chem. 17 (1978) 3334.
[31] A.A. Batista, M.O. Santiago, C.L. Donnici, I.S. Moreira, P.C. Helay, S.J. Berners-Price, S.L. Queiroz, Polyhedron 20 (2001) 2123.
[32] A.A. Batista, L.R.V. Olmo, M.R.M. Fontes, G. Oliva, J. Braz. Chem. Soc. 7 (1996) 257.